

Marcel KRZAN\*, Kazimierz. MALYSA\*

## **INFLUENCE OF FROTHER CONCENTRATION ON BUBBLE DIMENSIONS AND RISING VELOCITIES<sup>#</sup>**

*Received March 5, 2002, reviewed, accepted May 15, 2002*

Influence of  $\alpha$ -terpineol concentration on local and terminal velocities of bubbles, their dimensions and shapes was studied within solution concentration range  $1 \cdot 10^{-5}$  to  $1 \cdot 10^{-3}$  mole/dm<sup>3</sup>. Bubble behaviour was monitored using CCD camera with stroboscopic illumination and high speed camera Speedcam 512. Variations of the bubble local velocity and its deformation were determined as a function of distance from the capillary orifice and analysed in terms of adsorption coverage at interface of the departing bubble. Two kinds of dependencies of the bubbles local velocities on distance were observed. At low  $\alpha$ -terpineol concentrations the profiles of the bubble local velocity showed maximum at distances ca. 5-20 mm from the capillary orifice, prior to reaching a value of the terminal velocity. No maximum was observed at distilled water and  $\alpha$ -terpineol concentrations  $c > 0.0001$  mole/dm<sup>3</sup>. It was found that  $\alpha$ -terpineol adsorption coverage of ca. 6% was the minimum needed to assure the full immobilization of the bubble surface and the lowering of bubble terminal velocity by ca. 60% as result of it.

*Key words: bubble, rising velocity, frother,  $\alpha$ -terpineol, adsorption, surface coverage*

### **INTRODUCTION**

Frother is one of the main reagents applied in flotation processes and its essential task is to modify properties of the solution/gas interface and assure formation of a foam layer. According to Leja frother is also important in elementary act of flotation, i.e. in formation of the bubble-grain aggregates (Leja, 1956/57; Leja, 1982). Interactions between frother and collector molecules, during collisions in flotation cell of bubbles and grains, facilitate formation of stable bubble-grain aggregates. Importance of a proper choice of the frother and existence of the collector-frother interaction was later also discussed and documented in (Lekki and Laskowski, 1971; Laskowski, 1998; Bansal and Biswas, 1975; Malysa at al., 1981) amongst others.

---

\*Institute of Catalysis and Surface Chemistry Polish Academy of Sciences,  
ul. Niezapominajek, 30-239 Krakow, Poland

<sup>#</sup> This paper is dedicated to prof. A. Pomianowski on the occasion of his 80th birthday

In flotation bubbles act as carriers transporting grains of useful ore component(s) to froth layer. Probability of collision,  $P_k$ , of bubbles and grains depends on their dimensions (Laskowski, 1974; Reay and Ratckliff, 1973; Weber and Paddock, 1983; Yoon and Lutrell, 1989; Schimmoler et al. 1993) as:

$$P_k = A (R_g / R_b)^n \quad (1)$$

where  $R_b$  and  $R_g$  are the bubble and grain radius, respectively,  $A$  and  $n$  are parameters that vary with Reynolds' number of bubbles. For conditions representative for flotation  $n=2$  is generally assumed. As a result of frother adsorption the dimensions of bubbles formed during gas dispersing and their rising velocity can be changed. Degree of adsorption coverage at interface of the bubble formed depends mainly on velocity of creation of fresh gas/liquid interface and kinetics of frother adsorption. When the bubble formed starts to rise up its motion causes disequilibrium of the adsorption coverage along the bubble interface and a gradient of the frother surface concentration is induced (Levich, 1962; Dukhin and Deryaguin, 1961). This gradient of the surface concentration (surface tension) reduces mobility of the bubble interface and consequently the bubble velocity is lowered. Lower bubble velocity means a longer time of contact with colliding grains.

The paper presents results of studies on influence of  $\alpha$ -terpineol concentration on local and terminal velocities of bubbles, their dimensions and shapes. Profiles of the local velocities of bubbles in clean water and  $\alpha$ -terpineol solutions were determined as a function of distance from the capillary orifice on which the bubbles were formed. Variations of the bubble velocity and dimensions are analysed in a function of solution concentration and adsorption coverage at interface of the departing bubble, as well.

## EXPERIMENTAL

Figure 1 presents schematically the set-up used in the experiments. Bubbles were formed at the capillary orifice of inner diameter 0.07mm using the Cole-Parmer syringe pump enabling high precision control of the gas flow. To avoid optical distortions a square glass column (40x40 mm) was used to monitor velocity and dimensions of the bubbles departing from the capillary. Bubble motion was monitored and recorded over ca. 350mm distance from the capillary orifice. Sony XC-73CE CCD camera (with Cosmimar objective and rings for magnification) coupled with TV monitor and JVC BR-S800U professional video recorder (with Editing Control Unit RM-86U) were used to monitor and record the bubbles motion. To determine local velocity of the bubble at various distances from the capillary orifice a stroboscope (Drelloscope) illumination with 100-200 flashes per second was applied. In such manner 4-8 images of the bubble positions were obtained on each frame of the videotape. To get absolute dimensions an image of the nylon sphere of 7.85mm diameter was recorded after each experiment.

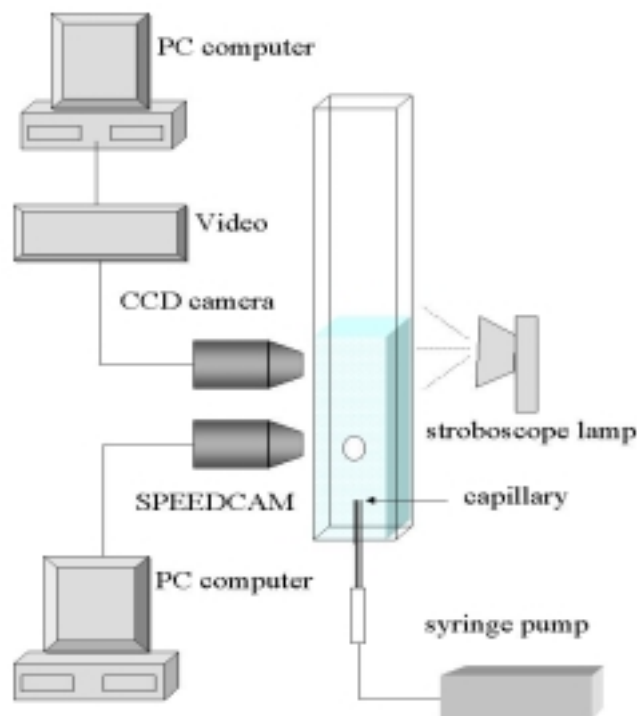


Fig.1. Schematic of the experimental set-up

Sequences of frames of the video recordings were digitalized using frame grabber and analyzed using a PC with SigmaScanPro Image Analysis Software. Distances between subsequent positions of the bubble on the frame and its vertical and horizontal diameters were measured as a function of distance from the capillary. Every measurement was performed at least 3 times and mean values were calculated.

High speed camera Speedcam 512+ was used to determine bubble behavior during acceleration, immediately after departing from the capillary, and at the stage of “collision” with free surface, i.e. at the bubble arrival at solution surface. The camera maximum speed is 1182 frames per second, i.e. it makes possible recording of phenomena occurring in time scale shorter than 1 msec (ca. every 850 microseconds).

Surface tension of  $\alpha$ -terpineol solutions was measured using the du Nouy ring method (Lauda tensiometer model TD 1), taking into account the necessary correction factors (du Nouy and Lectome, 1919; Lunkenheimer, 1982). The accuracy of the measurements was 0.1mN/m.

Four-times distilled water and commercial  $\alpha$ -terpineol was used for the solutions preparation. The experiments were carried out in room temperature ( $20\pm 1^\circ\text{C}$ ).

## RESULTS AND DISCUSSION

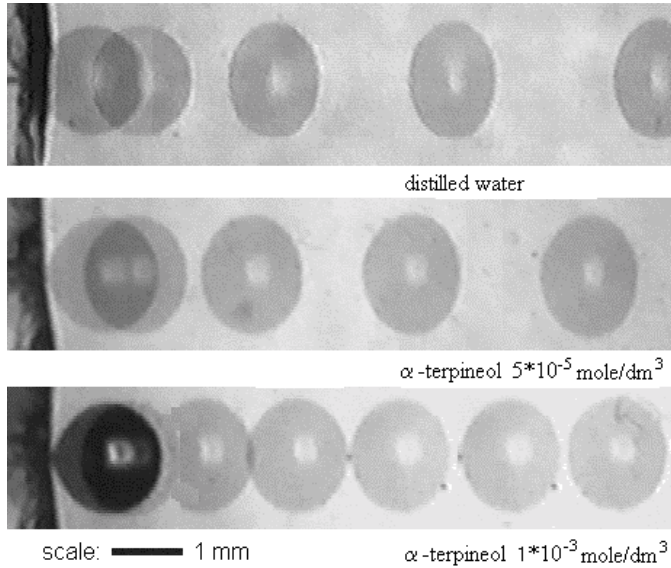


Fig.2. Images of bubbles departing from the capillary orifice at distilled water and  $\alpha$ -terpineol solutions of concentrations  $5 \cdot 10^{-5}$  and  $1 \cdot 10^{-3}$  mole/dm<sup>3</sup>.

Figure 2 presents the images of bubbles departing from the capillary orifice at distilled water and  $\alpha$ -terpineol solutions of concentrations  $5 \cdot 10^{-5}$  and  $1 \cdot 10^{-3}$  mole/dm<sup>3</sup>. A few important features can be noted immediately from these pictures. With increasing  $\alpha$ -terpineol concentration: i) the distances between consecutive images, ii) dimensions, and iii) deformations of the bubbles are decreasing. As these experiments were carried out under identical stroboscopic illumination (100 flashes/sec) it shows that the bubbles velocity was decreasing with increasing  $\alpha$ -terpineol concentration. It is seen also that the bubbles, which were spherical at the capillary orifice, underwent deformation immediately after departure and the deformation was the largest in clean water.

Variations of local velocities of bubbles with the distance,  $L$ , from the capillary orifice are presented in Fig. 3 for distilled water and  $\alpha$ -terpineol solutions of different concentrations. Local velocity,  $U$ , of the bubble was calculated from position of subsequent images of the bubble as:

$$U = \frac{\sqrt{(x_2 - x_1)^2 + (y_2 - y_1)^2}}{\Delta t} \quad (2)$$

where  $(x_2, y_2)$  and  $(x_1, y_1)$  are coordinates of the bubble positions, and  $\Delta t$  is the time interval between flashes of the stroboscopic lamp. Fig. 3A shows the velocity profiles in close neighbourhood of the capillary, i.e. for  $L < 40$  mm, while Fig. 3B for the distances up to 350mm. Immediately after departure the bubble velocity in distilled

water and  $\alpha$ -terpineol solutions increases rapidly. Next, at distances ca. 5-20 mm either a plateau value is attained or a maximum is observed. As seen in Fig. 3 at low  $\alpha$ -terpineol concentrations three stages can be distinguished on the  $U=f(L)$  dependences: i) a rapid acceleration of the bubble immediately after departure, ii) attainment a maximum value followed by a monotonic decreasing of the velocity, and iii) a constant value of velocity, which did not change with distance.

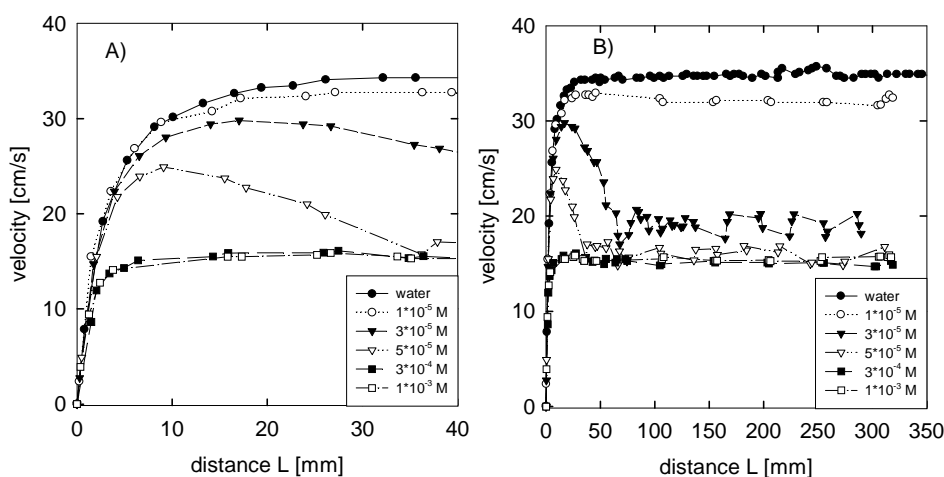


Fig. 3. Variations of local velocities of bubbles with the distance,  $L$ , from the capillary orifice. Part A - in the proximity of the capillary ( $L \leq 40$  mm), part B - for the distance  $L$  up to 350mm

This constant value of the bubble velocity is called the terminal velocity. With increasing  $\alpha$ -terpineol concentration the maximum height was diminishing and its position was shifted towards shorter distances  $L$ . In high concentrations of  $\alpha$ -terpineol solutions and in distilled water no maximum was observed and after period of rapid acceleration the bubbles attained the terminal velocity. The bubble terminal velocity was decreasing steadily with increasing  $\alpha$ -terpineol concentration, from  $34.8 \pm 0.3$  cm/s in distilled water down to  $15.4 \pm 0.03$  cm/s in  $0.001$  mole/dm<sup>3</sup>  $\alpha$ -terpineol solution.

Influence of  $\alpha$ -terpineol concentration on size of the bubbles formed at the capillary orifice is illustrated in Fig. 4. There are presented the bubble sizes determined experimentally and calculated. As was discussed above (see Fig. 2) the bubbles were not spherical and therefore the equivalent diameter ( $d_{eq}$ ), i.e. diameter of sphere having identical volume as the distorted bubble, was determined on a basis of measurements of the bubble vertical ( $d_v$ ) and horizontal ( $d_h$ ) diameters as:

$$d_{eq} = (d_v d_h^2)^{1/3} \quad (3)$$

Simultaneously the bubble diameters were measured at the capillary orifice, immediately before their departure. Line in Fig. 4 presents values of bubble diameters as calculated from the classical Tate's Law (a balance of the buoyancy and surface tension forces acting on the bubble) the bubble diameter is given as:

$$d_t = [6 d_o \sigma / (\Delta\rho g)]^{1/3} \quad (4)$$

where  $d_o$  is the inner capillary diameter,  $\sigma$  is the solution surface tension,  $\Delta\rho$  is the density difference and  $g$  is the gravity acceleration. As seen in Fig. 4 with increasing solution concentration the bubbles diameters were decreasing, but the changes were relatively small (ca. 10%), from  $1.48 \pm 0.03$  mm in distilled water to  $1.38 \pm 0.03$  mm in  $0.001$  mole/dm<sup>3</sup>  $\alpha$ -terpineol solution.

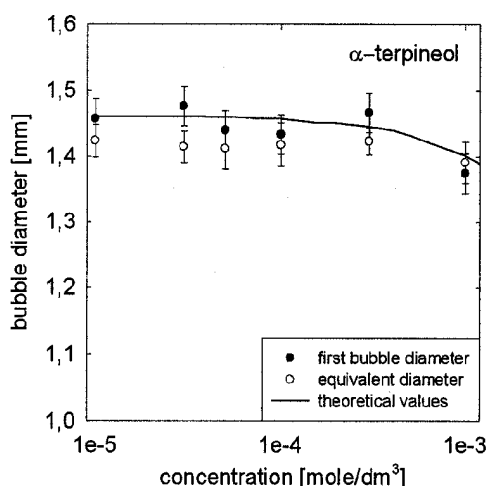


Fig. 4. Variations of the bubble diameter with  $\alpha$ -terpineol concentration

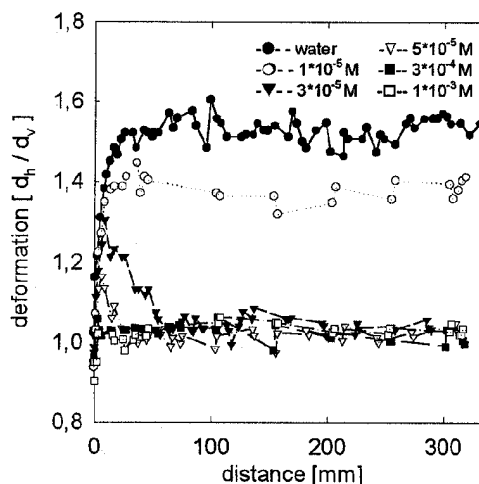


Fig 5. Variations of the bubble deformation with the distance,  $L$ , from the capillary orifice

Variations of the bubble shape deformation with distance  $L$  are showed in Fig. 5 for different  $\alpha$ -terpineol concentrations. Deformation from the spherical shape was determined from measurements of the horizontal and vertical diameters as a ratio of these diameters. As seen the bubbles, spherical on the capillary orifice, deformed almost immediately after departing. The maximum deformation was observed in a clean water. With increasing  $\alpha$ -terpineol concentration the deformations were decreasing, At high concentrations ( $c \geq 3 \cdot 10^{-4}$  mole/dm<sup>3</sup>) the deformations were very small, of an order ca. 5% only. Comparing data presented in Figs. 5 and 3 a correlation between variations of the bubble local velocities and its deformation can be noted. Maxima were observed for the same solution concentrations (lowest  $\alpha$ -terpineol

concentrations) and at similar distances from the capillary. Reasons of these phenomena will be discussed further.

To get information about degree of adsorption coversages the surface tension of  $\alpha$ -terpineol solutions was measured and values of the surface excess (surface concentration),  $\Gamma$ , were calculated. Fig. 6A presents the dependences of the surface tension,  $\sigma$ , and the  $\Gamma$  values on  $\alpha$ -terpineol concentration. Equation of state derived from the Frumkin isotherm:

$$\sigma = \sigma_0 + RT \Gamma_{\infty} \left[ \ln(1 - \theta) + \frac{H_s}{RT} \theta^2 \right] \quad (5)$$

where  $\sigma_0$  - is the surface tension of water,  $\theta = \Gamma/\Gamma_{\infty}$ ,  $\Gamma_{\infty}$  the maximum surface concentration and  $H_s$  is the Frumkin interaction parameter, was fitted to the dependencies of surface tension on concentration of the n-alkanols solutions studied. The obtained parameters of the Frumkin isotherm are as follows:  $\Gamma_{\infty} = 4.15 \cdot 10^{-10}$  mole/cm<sup>2</sup>,  $a_i = 1.21 \cdot 10^{-3}$  mole/dm<sup>3</sup>,  $H_s = 1.75$  kJ/mole. Points in Fig. 6A show the measured surface tension data, while line is the fitted dependence.

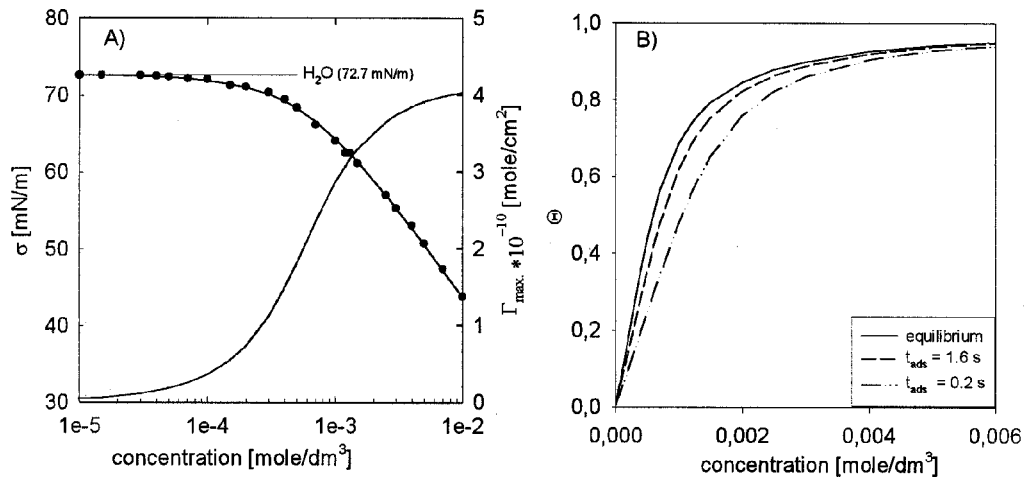


Fig. 6. A - Dependences of the surface tension,  $\sigma$ , and the surface excess,  $\Gamma$ , on  $\alpha$ -terpineol concentration. B - Values of the equilibrium adsorption coverage,  $\theta$ , and the adsorption coverage over surface of the departing bubbles for  $t_{ads} = 1.6$  and 0.2 sec as a function of  $\alpha$ -terpineol concentration

To determine adsorption coverage at the interface of the bubble detaching from capillary orifice in  $\alpha$ -terpineol solution the convective-diffusion model elaborated in (Warszynski at al., 1998) for the bubble detaching from capillary described in details in (Jachimska at al., 2001) was applied. In our experiments the time of rapid expansion of the bubble surface was 1.6 sec. It means that degree of adsorption

coverage over surface of the departing bubble was determined by amount of  $\alpha$ -terpineol adsorbed at the bubble interface during this time. Figure 6B presents values of the adsorption coverages over surface of the departing bubbles,  $\theta_{\text{dep}}$ , as a function of  $\alpha$ -terpineol concentration. For sake of comparison there are also presented the equilibrium adsorption coverages. As seen the adsorption coverages at interface of the departing bubble ( $t_{\text{ads}}=1.6$  s) were lower than the equilibrium ones ( $t_{\text{ads}}= \infty$ ). However, these deviations were not large – of an order 20-30% (maximum). Certainly, when the bubble formation time is shorter then the differences could be very significant. This is illustrated also in 6B (see data for  $t_{\text{ads}}= 0.2$ s).

In Fig. 7 the experimentally determined values of the bubble terminal velocities are compared to that ones predicted from the models available in the literature. Solid points show the terminal velocity values, while empty points refer to the maximum local velocities in  $\alpha$ -terpineol solutions. The dashed lines present values of the bubble terminal velocity in clean water as calculated from the Moore (1965) theory and the Clift at al. (1973) model. In the Moore theory the terminal velocity is calculated from a drag coefficient  $C_D$  of an oblate spheroid:

$$C_D = \frac{48G(\chi)}{\text{Re}} \left( 1 + \frac{H(\chi)}{\text{Re}^{\frac{1}{2}}} + \dots \right) \quad (6)$$

where  $\text{Re}$  is a Reynolds number and  $G$  and  $H$  are functions of the aspect ratio  $\chi$  defined as the ratio of the major and minor diameters of bubble).

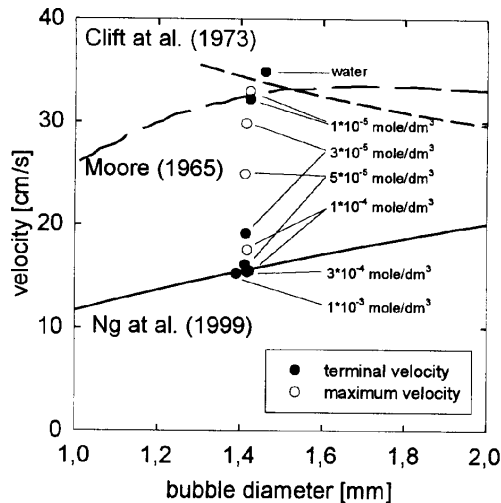


Fig.7. Comparisons of the experimental values, of the terminal (solid symbols) and maximum (empty symbols) velocities of bubbles in distilled water and  $\alpha$ -terpineol solutions, to predictions of the models

The terminal velocity  $U_t$  of bubble is calculated by an iteration procedure from the relation:

$$U_t \left(1 + \frac{H(\chi)}{Re^2}\right) = \frac{r^2 g}{9\nu G(\chi)} \quad (7)$$

where  $r$ ,  $g$ , and  $\nu$  and a bubble radius, a gravitation acceleration and viscosity, respectively. According to Clift at al. for bubbles of diameters  $d_e > 1.3$  mm their terminal velocity can be approximated line as:

$$U = [(2.14 \sigma / \rho d_e) + 0.505 g d_e]^{1/2} \quad (8)$$

The solid line shows velocity values as calculated from the equation:

$$U = 5450 \Delta \rho d^2 \left(\frac{7}{6} Re^{0.15} + 0.02 Re\right)^{-1} \quad (9)$$

(Ng at al., 1999) describing motion of a “contaminated” bubble, i.e. in a presence of surfactant.

A few important features can be noticed in Fig. 7. First, the bubble velocity measured in clean water was even a bit higher than that predicted by Moore (Eq. 7) and Clift at al. (Eq. 8) models describing bubble motion in clean liquids, what indicates that our water was really clean. Next, at high  $\alpha$ -terpineol concentrations the experimentally determined velocity values are in a good agreement with the „contaminated” model (Eq. 9) predictions. However, at low  $\alpha$ -terpineol concentrations ( $c < 0.0001$  mole/dm<sup>3</sup>) the experimental data are between the values predicted by the models for „clean” and „contaminated” bubbles. Models for motion of „clean” bubbles assume full fluidity of the bubble interface, while the „contaminated” ones assume that the bubble interface is fully immobilized („solidified”) as a result of surfactant adsorption. Results presented in Fig. 7 clearly show that there is needed a critical (minimum) degree of adsorption coverage to immobilize fully the bubble surface. In the case of  $\alpha$ -terpineol this minimum adsorption coverage needed is ca. 6%. When adsorption coverage is not high enough to retard motion at the bubble surface then its rising velocity can be very significantly higher (even 2 times). Empty points in Fig. 7 present values of the local velocity of bubbles at their maximum (see Fig. 3). In our opinion higher velocity of the bubbles having identical dimensions and rising in the same solution can be caused only by differences in the degree of immobilization of the bubble surface. It indicates also that at low solution concentration there is needed some time to develop a steady state distribution of the adsorbed surfactant, i.e. steady state surface tension gradients immobilizing interface of the accelerating bubble. This is confirmed by data presented in Fig. 5, which shows pulsations of the bubbles shape and are in a good correlation with variations of the bubble rising velocity with distance (see Fig. 3). When local values of surface tension over the bubble surface are changing the bubble shape is expected to pulsate.

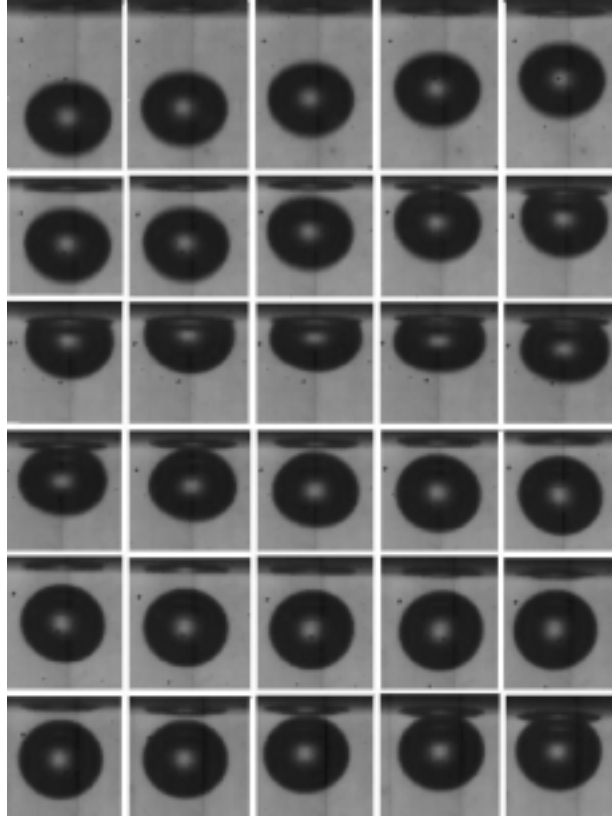


Fig. 8. Images of the bubble bouncing back to the solution from a liquid-gas interface. Time delay between the subsequent frames is 846  $\mu$ s

To illustrate how rapid are phenomena related to bubble motion and collisions a sequence of pictures of the bubble approaching surface of  $3 \cdot 10^{-5}$  mole/dm<sup>3</sup>  $\alpha$ -terpineol solution is presented in Fig. 8. Each subsequent picture shows the bubble position and its shape after a time interval of 0.845 ms. It is clearly seen that bubble approaching solution surface neither ruptures immediately nor „stays” at the surface. Velocity of the bubble approaching free surface didn't decrease till the surface started to be deformed. After forming a “dome” the bubble started to move backward, i.e. opposite to the direction of buoyancy force, within time period ca. 2-4 ms. Simultaneously, the bubble shape started to pulsate very rapidly, changing its shape during time intervals shorter than 0.845 ms. Number of these „bouncing” from solution surface and its distance varied with solution concentration.

These data show clearly, in our opinion, the importance of dynamic effects and non-equilibrium adsorption coverages in bubble motion, bubble collisions with grains and formation of the flotation aggregates.

## CONCLUSIONS

Adsorption of  $\alpha$ -terpineol at bubble surface causes significant decreasing of the bubble rising velocity. Even such low  $\alpha$ -terpineol concentration as  $3 \cdot 10^{-5}$  mole/dm<sup>3</sup> lowered the bubble terminal velocity by ca. 40%, from 34.8 to 19.1 cm/s. Depending on  $\alpha$ -terpineol concentration the bubbles showed 2 kinds of variations of the local velocity with distance from a point of their formation. At lowest  $\alpha$ -terpineol concentrations three stages; acceleration, deceleration and finally steady state (terminal velocity) were detected. At high concentrations only the first and last stage were observed, i.e. there was no maximum on the  $U_{\text{local}}=f(\text{distance})$  dependencies. It was showed that degree of adsorption coverage of the bubble surface by  $\alpha$ -terpineol molecules is the most important factor affecting bubble local velocity profiles and shape pulsations. It was found that adsorption coverage of ca. 6% was the minimum needed to assure a full immobilization of the bubble surface and as result of it the lowering of bubble terminal velocity by ca. 60%.

It was demonstrated that phenomena related to bubble motion, such as shape pulsations and collisions are very rapid (time scale of microseconds). It indicates that dynamic effects and lack of equilibrium adsorption coverages should always be taken into consideration in description of the bubble-grain collisions, formation of the flotation aggregates and their transport to froth layer.

## ACKNOWLEDGMENTS

Partial financial support from grant of State Committee for Scientific Research (KBN 4 T09A 058 22) is gratefully acknowledged. The authors thank Dr. P. Warszynski for program for calculations of the adsorption coverages and Eng. M. Baranska for her help in surface tension measurements.

## REFERENCES

- BANSAL V.K. AND BISWAS A.K., *Trans. IMM. Sect. C*, 84 (1975) 131-135. Clift R., Grace J.R. and Weber M.E., Academic Press New York San Francisco London 1978
- DUKHIN S.S., DERYAGUIN B.V., *Zh. Fiz. Khim.*, 35, (1961) 1246-1453.
- JACHIMSKA B., WARSZYŃSKI P., MALYSA K., *Colloids & Surfaces A*, 192 (2001) 177.
- LASKOWSKI J.S., in "Frothing in Flotation II" (Laskowski J.S. and Woodburn E.T.- Editors), Gordon and Breach Science Publishers, 1998, chap. 1, p. 1.
- LASKOWSKI J., *Miner. Sci. Eng.*, 6 (4), 223 (1974)
- LEJA J., *Trans. IMM.*, 66 (1956/57) 425-437.
- LEJA J., *Surface Chemistry of Froth Flotation*. Plenum Press, New York and London, 1982, chap. 9, p. 549.
- LEKKI J. and Laskowski J.S., *Trans. IMM. Sect. C*, 80 (1971) 174-180.
- LEVICH V.G., *Physico Chemical Hydrodynamics*, Prentice Hall., (1962)
- LUNKENHEIMER K., *Tenside Detergents*, 19 (1982) 272-281.
- MALYSA K., BARZYK W. AND POMIANOWSKI A., *Int. J. Mineral Process.*, 8 (1981) 329-343.
- MOORE D.W., *J. Fluid Mechanics*, 23 (1965) 749-766
- NG S., WARSZYŃSKI P., ZEMBALA M., MALYSA K., *Physicochemical Problems of Mineral Processing*, 33(1999) 143-161
- du NOUY, P. LECOMTE, *J.Gen. Physiol.*, 1 (1919) 521.

- REAY D., RATCKLIFF G.A., *Can. J. Chem. Eng.* 52, 178 (1973)  
SCHIMMOLER B.K., LUTRELL G.H., Yoon R.-H., *Proc. XVIII Intern. Miner. Process. Congress, Sydney, 23-28 May, Vol. 3, 263* (1993)  
WARSZYŃSKI P., WANTKE K.-D., FRUHNER H., *Colloids & Surfaces A*, 139 (1998) 137.  
WEBER M.E., PADDOCK D., *J. Coll. Interface Sci.*, 94 (2), (1983)  
YOON R.-H., G.H. LUTRELL G.H. (1989), *Mineral Process. Extractive Metall. Review*, 5, 101.

**Krzan M., Małysa K.,** *Wpływ stężenia odczynnika pianotwórczego na rozmiary i prędkości lokalne bąbelczek gazu*, *Fizykochemiczne Problemy Mineralurgii*, 36, (2002) 65-76 (w jęz. ang.)

Badano wpływ stężenia  $\alpha$ -terpineolu na prędkości lokalne i graniczne bąbelki, ich rozmiar oraz deformację kształtu. Wyznaczono profile prędkości lokalnych bąbelki i kształtów w funkcji odległości od kapilary ( $\varphi=0.07\text{mm}$ ) na której wytwarzano bąbelki przy pomocy precyzyjnej pompy strzykawkowej. Pomiarów wykonano dla roztworów  $\alpha$ -terpineolu w zakresie stężeń od  $1\cdot 10^{-5}$  do  $1\cdot 10^{-3}$  mole/dm<sup>3</sup>. Ruch bąbelki był monitorowany za pomocą dwóch kamer, zbierających informacje o położeniu i kształcie z częstotliwościami 100 i 1182 Hz. Stwierdzono występowanie kilku różnych etapów w ruchu bąbelki wpływających w roztworach  $\alpha$ -terpineolu. Bąbelki bezpośrednio po oderwaniu od kapilary przyspieszają, po czym w zależności od badanego stężenia ich prędkości osiągają stałą wartość graniczną (woda i roztwory  $\alpha$ -terpineolu o dużym stężeniu) lub też obserwowane jest przejście przez maksimum i stopniowe spowolnienie prędkości do innej, często znacznie mniejszej niż maksymalna, wartości prędkości granicznej (stężenia mniejsze od 0.0001 mol/dm<sup>3</sup>). W przypadkach niskich stężeń równocześnie ze zmianami profili prędkości lokalnych są obserwowane dynamiczne zmiany kształtu bąbelki. Wartości prędkości granicznych unoszących się bąbelki spadają wraz ze wzrostem stężenia  $\alpha$ -terpineolu od  $34.8\pm 0.03$  cm/s w wodzie destylowanej do  $15.4\pm 0.03$  cm/s w roztworze  $\alpha$ -terpineolu o stężeniu 0.001 mol/dm<sup>3</sup>.

Stwierdzono, że stopień pokrycia adsorpcyjnego na powierzchni bąbelki jest czynnikiem decydującym o profilach prędkości lokalnych bąbelki, jak i ich deformacjach. Największe zmiany występują w obszarze niskich stężeń  $\alpha$ -terpineolu, przy których stopień pokrycia adsorpcyjnego zmienia się w zakresie 0-10%. Pokrycie adsorpcyjne  $\alpha$ -terpineolem  $\Theta=6\%$  jest minimalnym pokryciem niezbędnym dla całkowitego unieruchomienia powierzchni bąbelki w wyniku którego graniczna prędkość bąbelki ulega znacznemu zmniejszeniu.